

Submitted: ApJ, Sept. 2008; revised Nov. 25, 2008

The Cepheid Distance to NGC 0247

Barry F. Madore & Wendy L. Freedman

The Observatories
Carnegie Institution of Washington
813 Santa Barbara Street
Pasadena, CA 91101
email: barry@ociw.edu, wendy@ociw.edu

Joseph Catanzarite

Jet Propulsion Laboratory, MS 301-486
480 Oak Grove Dr.
Pasadena, CA 91109-8099
email: joseph.h.catanzarite@jpl.nasa.gov

Mauricio Navarrete

Las Campanas Observatories
Carnegie Institution of Washington
La Serena, Chile
email: mnavarrete@lco.cl

ABSTRACT

We report VRI CCD observations of nine Cepheids in the South Polar (Sculptor) Group spiral galaxy NGC 0247. Periods of these Cepheids range from 20 to 70 days. Over the past 20 years the very brightest Cepheid in our sample, NGC 0247:[MF09] C1, has decreased its period by 6%, faded by 0.8 mag in the V band, and become bluer by 0.23 mag in (V-I). A multi-wavelength analysis of the Cepheid data yields a true distance modulus of $\mu_o = 27.81 \pm 0.10$ mag (3.36 \pm 0.16 Mpc) with a total line-of-sight reddening of $E(V-I) = 0.07 \pm 0.04$ mag, after adopting an LMC true distance modulus of 18.5 mag and reddening of $E(B-V) = 0.10$ mag. These results are in excellent agreement with other very recently published (Cepheid and TRGB) distances to NGC 0247. Combining both Cepheid datasets gives $\mu_o = 27.85 \pm 0.09$ mag (3.72 \pm 0.15 Mpc) with $E(V-I) = 0.11 \pm 0.03$ mag.

Subject headings: Cepheids: galaxies: distances and redshifts — galaxies: individual (NGC 0247) — galaxies: Sculptor Group

1. Introduction

In 1983 we began a ground-based project to provide a more secure calibration of the zero-point for secondary distance indicators (such as the Tully-Fisher relation) by building up a database of accurate Cepheid distances to nearby spiral galaxies. In due course the Hubble Space Telescope was launched and other activities took precedence over the ground-based effort. Preliminary mention of work on Cepheids discovered in NGC 0247 was given in Freedman et al. (1988) and again in Catanzarite, Freedman, Horowitz & Madore (1994) but details were never published, until now. Here we present the photometric data and provide a brief analysis leading to a distance determination to NGC 0247 based on nine Cepheids discovered in NGC 0247 some twenty-five years ago. We then go on to compare it with new observations published by Garcia-Varela et al. (2008, hereafter [GV08]).

2. Observations

Observations for this program were carried out over a span of eight years (giving a time baseline of almost 3,000 days). Observing began first at the Cerro Tololo 4m, and was completed using the 2.5m duPont telescope at Las Campanas, Chile. Three fields of NGC 0247 were surveyed in B , V , R , and I filters at the Cerro Tololo 4m telescope during November 1984 to November 1988. Figure 1 shows a photograph of NGC 0247 with the three fields delineated. The coordinates of the CCD field centers are given in Table 1. From the second through the fourth year of the program data were obtained in the service-observing mode offered at CTIO; those data were taken by M. Navarrete. For most of the runs the 512×320 RCA chip #5 (having a scale of 0.60 arcsec/pxl and a total field of view of $3'$ by $5'$ at the prime focus) was used. In 1988 a different RCA chip (#4) with similar characteristics was substituted. Exposure times for these frames were typically 400 sec in B and 300 sec in V , R and I . The frames were bias-subtracted, flat-fielded, and defringed using standard data-reduction packages available at Cerro Tololo. Beginning in 1990, the observing program for the Sculptor galaxies shifted to the duPont 2.5m telescope at the Las Campanas Observatory. $BVRI$ CCD observations covering the same three selected fields were obtained in December 1990, in September 1991, and in October, November, and December 1992. Exposure times at this telescope were generally 900 sec in B and 600 sec in V , R and I . Most of these observations were electronically binned (2×2) at the

telescope. For the 1990 and 1991 runs, the FORD1 CCD chip was used. For the October and November 1992 runs a Tektronix CCD chip (TEK4) was used; for the December 1992 runs, Tektronix CCD chips were also used (TEK3 and TEK4). These chips each had dimensions of 2048×2048 pixels; the image scales obtained were: FORD1: 0.16 arcsec/pxl; TEK3: 0.23 arcsec/pxl; and TEK4: 0.26 arcsec/pxl. The survey totalled about 250 exposures on 29 different nights over a span of eight years. Table 2 gives a journal of the observations.

3. Photometry Reduction and Calibration

Photometric calibration of the CTIO frames was accomplished using E-region standards in E1, E2, E3, E7, E8, and E9 (Graham 1984) and in SA 98 (Landoldt 1983). *BVRI* standards were taken on 20 independent photometric nights. As described in Freedman et al. (1992), a check on the external accuracy of the photometric calibration for these runs was made by individually calibrating the frames for NGC 0300. The magnitudes for the brightest stars were in agreement to within $0.01\text{-}0.03 \pm 0.03$ mag of the average for all filter/field combinations.

The CCD frames from CTIO were reduced using both DoPHOT (Schechter, Mateo & Saha 1993) and DAOPHOT (Stetson 1987), and cross-checked. The unresolved background level in NGC 0247 is highly non-uniform, and is characterized both by regions in which there are strong spiral arms as well as relatively blank, interarm regions. In order to maximize the detection limits of the algorithm FIND in DAOPHOT, the frames were first median-smoothed using a 7×7 pixel boxcar averaging scheme, and subtracted from the original frames.

Details of the calibration process are discussed in (Freedman et al. 1992). The LCO data were reduced using a variant of the DoPHOT package (Mateo & Schechter 1989). This version of DoPHOT uses median smoothing to construct an initial model of the background sky before searching for objects. The sky model is refined after objects at the next-to-the-lowest threshold have been found and subtracted. The refined sky model is then adopted as the baseline, and objects are again found down to the lowest threshold and their PSF parameters re-measured. LCO frames were brought onto the CTIO calibrated magnitude system by the following process: The $(B - V)$ color term for the CCD chips used at LCO relative to RCA chip used in the CTIO observations was measured and a correction was applied to the LCO B photometry (the LCO V photometry had no significant $(B - V)$ color term.) Next, the magnitude zero-point of each LCO frame was offset to the instrumental zero-point of a fiducial CTIO frame, for the corresponding field and filter. The calibration transformation derived for the fiducial CTIO frame was then applied to the LCO data.

4. The Cepheids

For Fields 1 and 3 all of the observations were tied to the photometric zero point for October 7, 1988. Observations on this night were taken under excellent seeing conditions and had the best photometric calibration available to us. For Field 2, October 13, 1988 was used to calibrate the data. To put all of the stars in each field on the same coordinate system, all frames from each field were spatially registered to the October 7, 1988 V frame for that field, (since that was the best or close to best V night for all three fields). Coordinate transformations produced matches with *rms* scatter of ± 0.30 pixels or better. Calibrated, matched photometry files containing the entire set of observations for each field/bandpass combination were produced. Stars with high internal V magnitude dispersion were then identified as described in (Freedman et al. 1994). These variable candidates were then subjected to a further test: a star was flagged as a Cepheid candidate only if the histogram of its magnitudes was consistent with a uniform magnitude histogram, as expected for Cepheids. All three fields were searched for variables down to a signal-to-noise level of 1.5σ . The V photometric data for each candidate was then phased to the twelve periods (in the range of 1 to 100 days) with the lowest phase dispersions, using a routine based on the Lafler-Kinman algorithm ((Lafler & Kinman 1965)). The V light curves were then visually inspected and the best period was selected. Calibrated B , R , and I observations were then phased to this adopted period and the multi-wavelength light curves were inspected for consistency. Candidates with strong correlation of phase and amplitude between their $BVRI$ light curves, having well-determined periods, mean colors and well-sampled light curves characteristic of known Cepheids were then identified as Cepheids. Each of these stars was then visually inspected in the best image frame to check for nearby companions. Nine Cepheids in total made it through the selection procedure. All were found in $BVRI$, with the exception of NGC 0247:[MF09] C9, which was too faint to be recovered on the I frames. The positions for the nine Cepheids in our sample are given in Table 3, the first 6 of which are mapped over from [GV08], with the positions for C7, C8 and C9 being on that system but having lower precision. The individual Cepheid observations are presented in Tables 4 through 12. The light curves are shown in Figure 2. The time-averaged properties of the individual Cepheids are listed in Table 4.

4.1. Other Variable Stars Found in NGC 0247

Five variable stars which could not be classified as Cepheids were also discovered. These stars are well-isolated, their photometry is well-measured by DoPHOT, and they have extremely strong $BVRI$ correlation. Three of them are very red, and have light curves with a

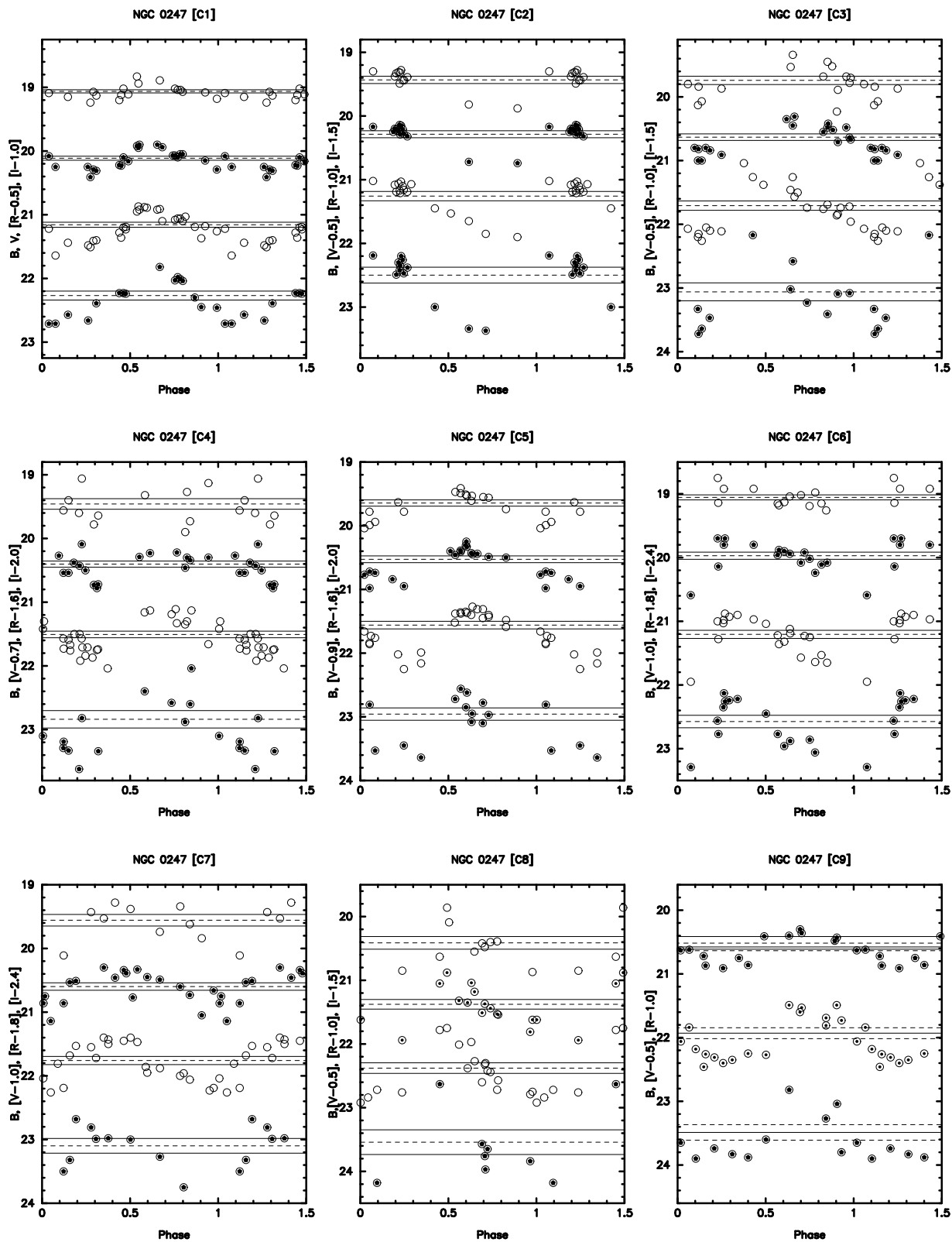


Fig. 1.— *BVRI* lightcurves for the individual Cepheids. The plotted magnitude range is 5 mag in all cases. Magnitude offsets, applied, to make the lightcurves individually more visible, are given in the vertical-axis labels. In order from top to bottom the lightcurves are *I*, *R*, *V* and *B*.

“square wave” shape. If they are eclipsing variables then we have probably been unable to determine the periods correctly. A fourth object has a light curve with the right shape to be a Cepheid, but is extremely red. The fifth may be a Cepheid with an uncharacteristic light curve. The properties of these stars are summarized in Table 13.

5. The Distance to NGC 0247

A comprehensive review of previously published distance estimates to NGC 0247 is given in [GV08].¹ In that paper the authors also present their new VI observations of 23 Cepheids in the period range 17 to 131 days. Based on those two colors they derive a true distance modulus of 27.80 ± 0.09 mag (3.6 Mpc) tied to an LMC true distance modulus of 18.50 mag, as also adopted in this paper. Another important independent distance measurement to NGC 0247 worth noting here, because of its comparably high precision, is the tip of the red giant branch (TRGB) distance modulus ($\mu_o = 27.81$ mag or 3.65 Mpc) published by Karachentsev et al. (2006).

5.1. Discussion of Data

The detected Cepheids at B lie closer to the photometry limits than at V , R , or I ; furthermore deriving a stable zero-point for that bandpass was found to be problematic. As such, the B data were used to confirm the periods adopted here, but because of signal-to-noise and other calibration problems we do not use the B -band data further in this paper. The B -band data are listed in this paper, but readers are strongly warned against using it for anything quantitative until a proper calibration is found. The time-averaged data for our 9 Cepheids are given in Table 14. The periods cited there were derived from these data alone, but will be updated later in the paper when we consider a merger with the [GV08] sample.

As can be seen in Figure 12, the NGC 0247 PL relations in V , R , and I , have smaller observed dispersions than the fiducial LMC PL relations whose 2-sigma widths are shown by the dashed lines. The small observed dispersion is presumably due to small number statistics, but it could also be signalling a slight bias in the sample. If the instability strip

¹In addition, an updated, on-line compilation of distances to nearby galaxies, including NGC 0247, is available through the *NASA/IPAC Extragalactic Database* at the following URL: <http://nedwww.ipac.caltech.edu/level5/NED1D/intro.html>.

is not being fully sampled we cannot be sure that these Cepheids properly reflect the mean. An external check with the results of [GV08] (Section 6 below) would suggest that that bias (between samples) is at or below the 0.1 mag level.

5.2. PL Relations and Apparent Distance Moduli

To determine apparent VRI distance moduli, residuals about the PL relations for NGC 0247 Cepheids were minimized relative to the mean LMC PL relations given in (?), and updated to the VI calibration of Udalski (2000). For a given bandpass, the LMC PL relation was iteratively shifted relative to the NGC 0247 PL relation until the χ^2 of the fit was minimized. The off-set determined in this way is then the apparent distance modulus (for that bandpass) of NGC 0247 with respect to the LMC. The results of the PL-fits are shown in Figure 3. In the absence of other physical effects, determination of the true distance modulus and reddening can be obtained by fitting the apparent moduli in different filters to an interstellar extinction law (e.g., Cardelli et al. 1989)² originally discussed in Freedman (1998).

In Figure 4, the apparent distance moduli at VRI for the Cepheid sample in NGC 0247 are plotted with respect to inverse wavelength. The solid line gives a fit to a standard (1) Galactic extinction law flanked by one-sigma error curves (dashed lines). The VRI data are very well-fitted by an extinction curve (with a small positive reddening equivalent to $E(V-I) = 0.07$ mag)³ having an intercept corresponding to a true distance modulus of $\mu_o = 27.81 \pm 0.10$ mag (3.65 ± 0.16 Mpc). The solution using only V and I gives essentially the same numbers ($\mu_o = 27.79 \pm 0.13$ mag; 3.61 ± 0.23 Mpc).

6. Comparison with Garcia-Varela et al. (2008)

We have made a positional cross-correlation of our Cepheids with those discovered by [GV08]. Six of our nine variables were recovered by the Araucania Project, and the correct identification of these stars across the two studies is reinforced by the independently derived

²Here we use $A_V = 3.2 \times E(B-V)$ and $A_V = 2.45 \times E(V-I)$. [GV08] choose to use a slightly different reddening law, taken from Schlegel et al. (1998), giving $A_V = 2.50 \times E(V-I)$ which is only 2% different from our adopted value.

³All reddenings in this paper are given in terms of $E(V-I)$. For those wishing the $E(B-V)$ equivalent the appropriate conversion factor is $E(B-V)/E(V-I) = 2.45/3.20 = 0.77$

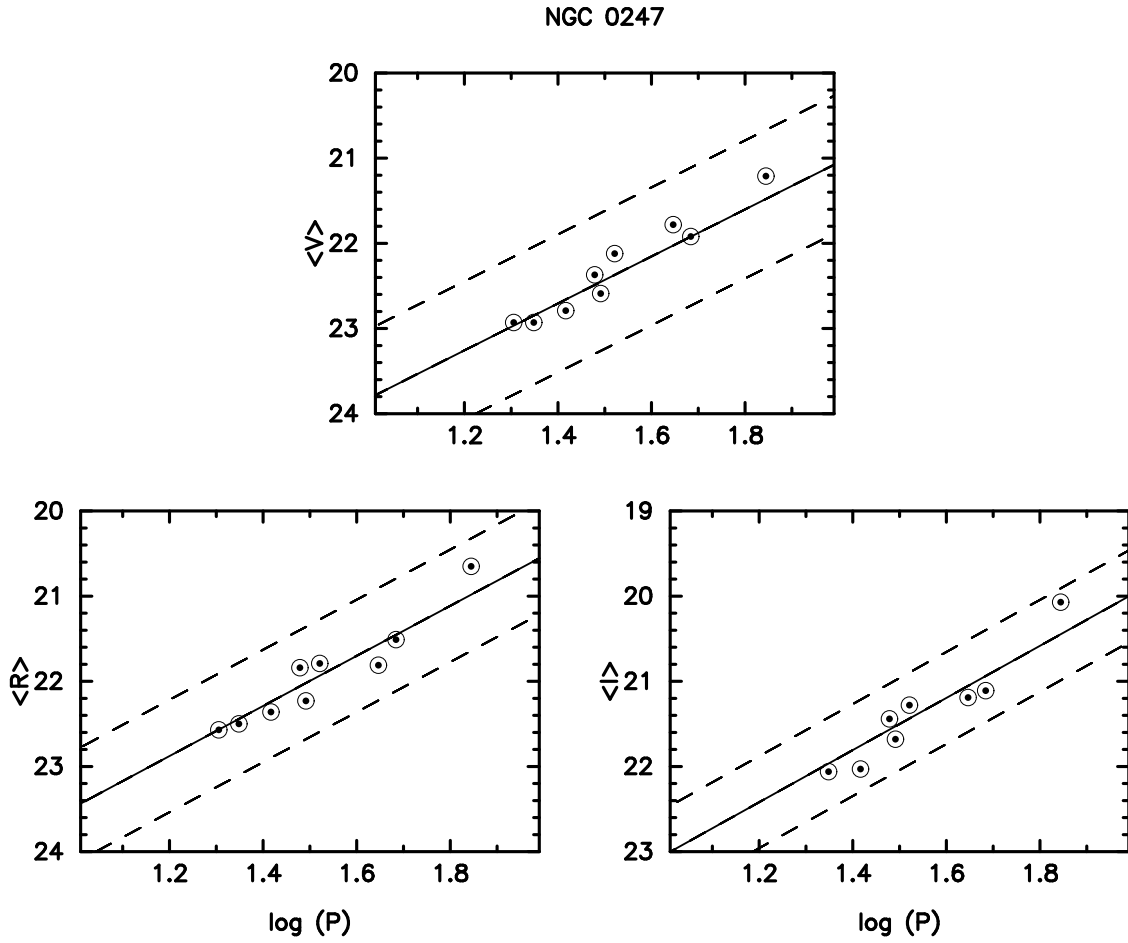


Fig. 2.— Fits of the NGC 0247 Cepheid PL-relations in V , R , and I to the LMC PL-relation. Solid lines show the least-squares fit, flanked by ± 2 -sigma boundaries to the instability strip as derived from LMC calibrators.

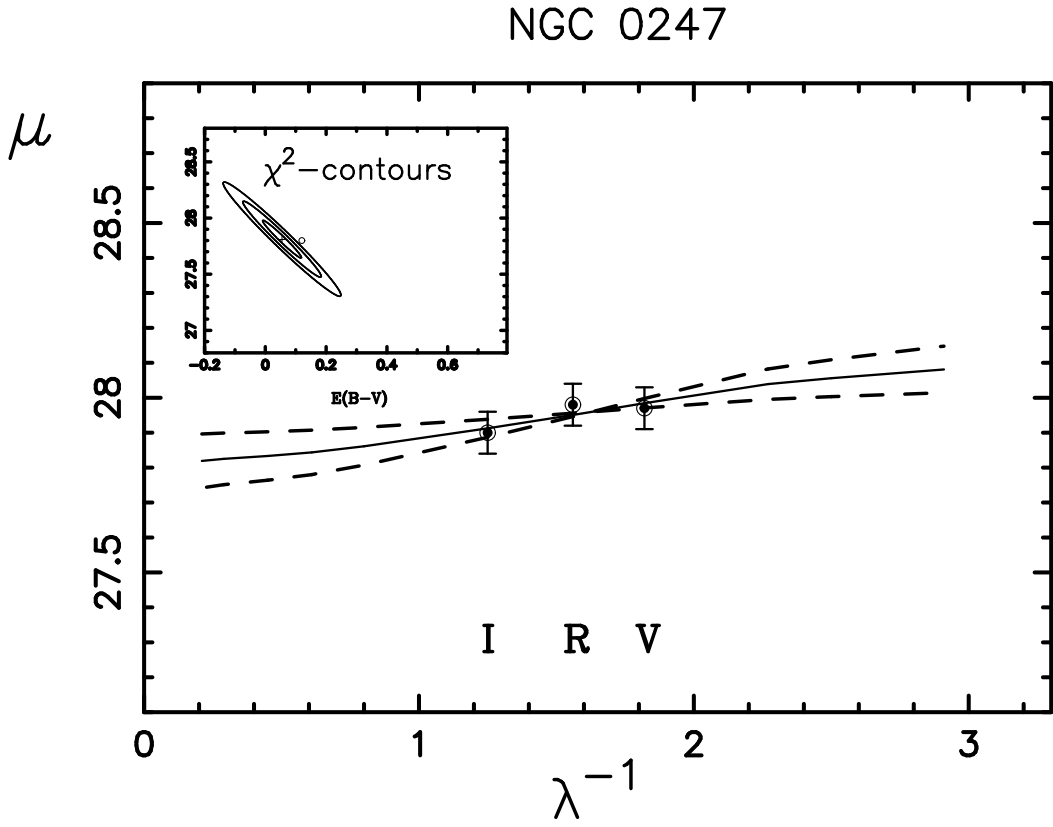


Fig. 3.— Fit of the apparent distance moduli in V , R , and I to a Galactic extinction law (solid line). One-sigma errors on the fit are shown with broken lines. Plotted contours are 2, 4 and 6 sigma.

periods which agree to better than 10% in most cases. We now combine the two datasets, revise the periods when possible and update the V and I intensity-mean magnitudes. The results of that update are given in Table 15. The combined lightcurves are shown in Figure 5.

The updated VRI [MF09] sample alone gives $\mu_V = 27.97 \pm 0.05$ mag, $\mu_R = 27.98 \pm 0.06$ mag, $\mu_I = 27.90 \pm 0.06$ mag, $E(V-I) = 0.11 \pm 0.03$ mag resulting in $\mu_o = 27.81 \pm 0.05$ mag or 3.65 ± 0.08 Mpc for the 3-band fit, and $\mu_o = 27.79 \pm 0.13$ mag (3.61 ± 0.23 Mpc) with $E(V-I) = 0.07 \pm 0.04$ mag for the VI fit alone.

We consider a progressive merger of the two datasets. We first apply our standard fitting techniques to the [GV08] preferred subset of 17 Cepheids, omitting as they did, the longest and shortest-period Cepheids in their sample. We get $\mu_V = 28.21 \pm 0.05$ mag, $\mu_I = 28.05 \pm 0.06$ mag, $E(V-I) = 0.15 \pm 0.03$ mag resulting in $\mu_o = 27.82 \pm 0.08$ mag or 3.66 ± 0.14 Mpc. This differs from the [GV08] solution by $+0.025$ mag in the true modulus.

If we now update the [GV08] sample with the revised periods and magnitudes for NGC 0247:[MF09] C2 through C6 we get $\mu_V = 28.15 \pm 0.06$ mag, $\mu_I = 28.03 \pm 0.06$ mag, $E(V-I) = 0.11 \pm 0.03$ mag resulting in $\mu_o = 27.87 \pm 0.09$ mag or 3.75 ± 0.15 Mpc. Augmenting the [GV08] sample with NGC 0247:[MF09] C7 & NGC 0247:[MF09] C8, plus reintroducing NGC 0247:[MF09] C1 with its first-epoch period and magnitude, in addition to its evolved values from [GV08] as described in Section 7 (below), we get $\mu_V = 28.13 \pm 0.05$ mag, $\mu_I = 28.01 \pm 0.06$ mag, $E(V-I) = 0.11 \pm 0.03$ mag resulting in $\mu_o = 27.85 \pm 0.09$ mag or 3.72 ± 0.15 Mpc. The above results are summarized in Table 16.

7. The 70-Day Cepheid NGC 0247:[MF09] C1

In an attempt to update the period and combine the photometry for the longest-period Cepheid in our sample, NGC 0247:[MF09] C1, we quickly found that the mean magnitudes and colors derived from our data did not correspond to data published for it in the [GV08] study. Figure 6 shows the differences. In that plot our data are shown as circled solid symbols, phased to our adopted period of 69.9 days. Below those light curves are the data from [GV08], shown as open circles, phased to their period of 65.862 days (with an arbitrarily added phase shift of 0.6 to align the lightcurves for ease of visual comparison). The time-averaged V magnitudes differ by 0.8 mag, with the most recent epoch being fainter; while the $(V-I)$ colors differ by 0.23 mag, with the most recent data being bluer. The sense of the change eliminates a self-shrouding event as the possible cause. A remaining explanation

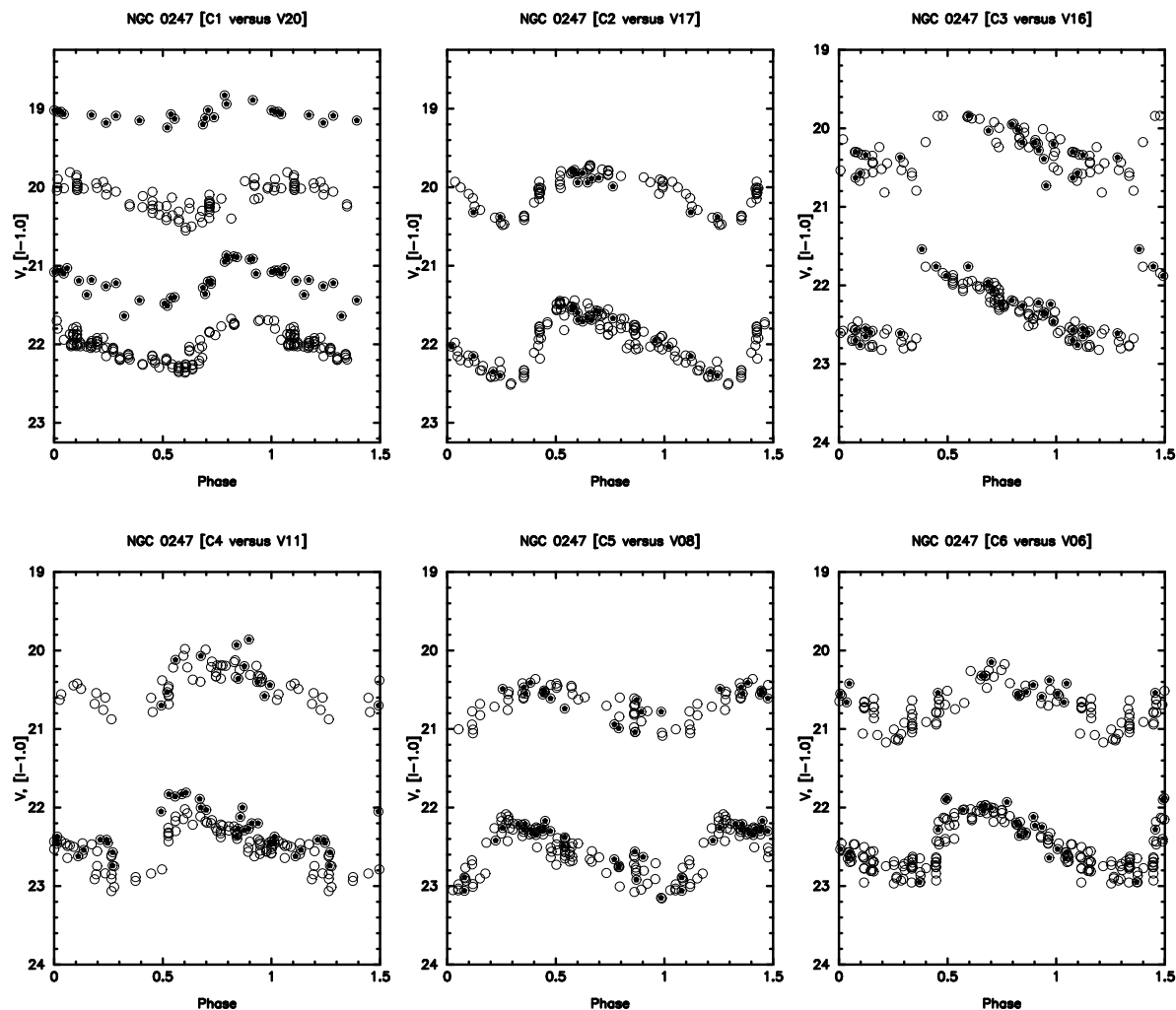


Fig. 4.— Combined $BVRI$ lightcurves for the individual Cepheids in NGC 0247. The plotted magnitude range is 5 mag in all cases. Magnitude offsets, applied, to make the lightcurves individually more visible, are given in the vertical-axis labels. In order from top to bottom the lightcurves are I , R , V and B . Solid points are from this paper; open circles are from [GV08].

is that the structure of the star itself may have systematically changed in the intervening quarter century: in the face of a rising surface temperature (indicated by the decrease in the (V-I) color) and the resulting increased surface brightness, the overall radius of this star may have decreased significantly. In the process the period dropped by 6%, from 70 to 66 days.

A simple linear decrease of the period with time ($\Delta P/P = 0.0075$ day/day) fails to phase the lightcurves over the total baseline (and, in fact, destroys coherence within the individual observing campaigns). Without undertaking more sophisticated modelling we default to the next simplest conclusion that the period change was a discontinuous event. Further monitoring of this star could reveal interesting aspects of the structure of Cepheids in general if this behavior persists.

8. Summary and Conclusions

Nine Cepheids have been identified in the Galaxy NGC 0247. Six of these variable stars have been independently found by [GV08].

The period and magnitude-updated VRI [MF09] sample alone gives apparent moduli of $\mu_V = 27.97 \pm 0.05$ mag, $\mu_R = 27.98 \pm 0.06$ mag, $\mu_I = 27.90 \pm 0.06$ mag, and $E(V - I) = 0.11 \pm 0.03$ mag resulting in $\mu_o = 27.81 \pm 0.05$ mag or 3.65 ± 0.08 Mpc for the 3-band fit. These data yield a true distance modulus of $\mu_0 = 27.70 \pm 0.11$ mag corresponding to a metric distance of 3.47 ± 0.18 Mpc.

Combining our observations with newly published data from [GV08] in the V & I bands, and updating the periods accordingly, results in a reddening of $E(V-I) = 0.06 \pm 0.04$ mag and a (preferred) true modulus of $\mu_0 = 27.81 \pm 0.05$ mag (3.65 ± 0.08 Mpc). This is (fortuitously) identical to the TRGB distance modulus recently published by Karachentsev et al. (2006) further re-inforcing the consistency of these two distance scales, which are based on largely independent assumptions, and have very different systematics.

The 70-day Cepheid NGC 0247:[MF09] C1 deserves follow-up observations to see if the extraordinary changes in its magnitude, period and color found between these epochs (first 1984-1992 and then 2002-2005) is an on-going phenomenon.

During the initial period in which these observations were made WLF's research was supported in part by NSF Grants AST 87-13889 and 9116496 on the extragalactic distance scale. We thank Bob Williams who provided us with Director's Discretion Time in 1988, and Irwin Horowitz who participated in the early stages of reducing the Las Campanas data.

NGC 0247 [C1 versus V20]

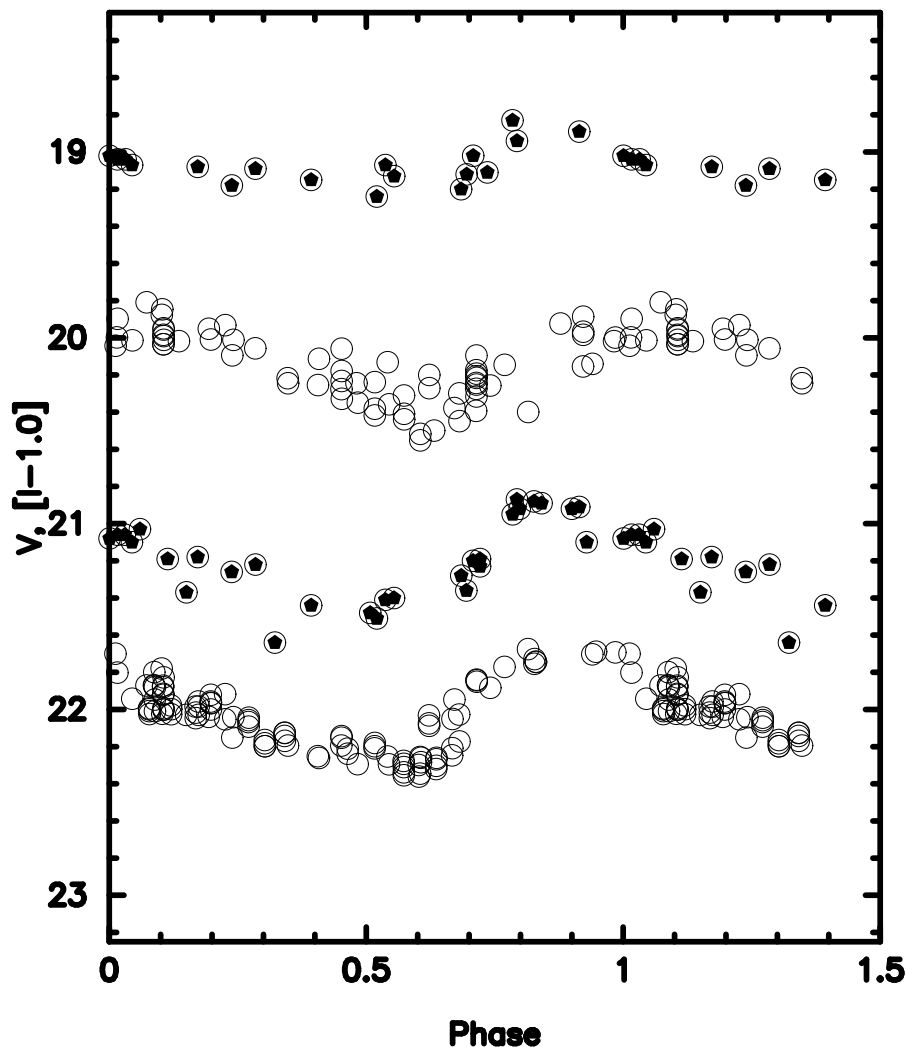


Fig. 5.— The V and I lightcurves for the Cepheid C1 at the two epochs surveyed by [MF09] (circled solid symbols) and [GV08] (open circles). The I-band light curves are both displaced by one magnitude upward in the figure for ease of viewing. In addition the earlier data are displaced in phase by 0.6 cycles so as to align the two datasets around maximum light. The data are phased to a period of 69.9 days for the [MF09] observations, and to a period of 65.862 days for the [GV08] observations. The vertical displacement of the pairs of light curves in V and in I is real, indicating that the star faded by nearly 0.8 mag between the times of the two studies.

We also thank Jose Garcia-Varela, Grzegorz Pietrzynski and Wolfgang Gieren for providing their more recently acquired Cepheid data in advance of publication. This research has made use of the NASA/IPAC Extragalactic Database (NED) which is operated by the Jet Propulsion Laboratory, Caltech, under contract with the National Aeronautics and Space Administration.

REFERENCES

- Cardelli, J.A., Clayton, G.C., & Mathis, J.S. 1989, *ApJ*, 345, 245
- Catanzarite, J., Freedman, W.L., Horowitz, I., & Madore, B.F. *BAAS*, 26, 1351
- Freedman, W.L., Madore, B.M., Hawley, S.L., Horowitz, I.K., Mould, J., Navarrete, M., & Sallmen, S. 1992, *ApJ*, 396, 80
- Freedman, W.L. 1988, *ApJ*, 326, 691
- Freedman et al. 1994, *ApJ*, 427, 628
- Garcia-Varela, A., et al. 2008, *AJ*, (accepted, arXiv:0808.3327)
- Graham, J.A. 1984, *AJ*, 89, 1332
- Karachentsev, I. et al. 2006, *AJ*, 131, 1361
- Lafleur, J., & Kinman, T.D. 1965, *ApJS*, 11, 216
- Landoldt, A. 1983, *AJ*, 88, 439
- Madore, B.F., (ed.) 1985, *IAU Colloq. 82, Cepheids: Theory and Observations*, (Cambridge Univ. Press), 166
- Mateo, M., & Schechter, P.L. in: *Proc. ESO Conf. Workshop 31, 1st ESO/ST-ECF Data Analysis Workshop*, ed. P.J. Grosbol, F. Murtagh, & R.H. Warmels, (1989 Garching: ESO), 69
- Schechter, P.L., Mateo, M., & Saha, A. 1993, *PASP*, 105, 1342
- Schlegel, D.J., Finkbeiner, D.P., & Davis, M. 1998, *ApJ*, 500, 525
- Stetson, P.B. 1987, *PASP*, 99, 191
- Udalski, A. 2000, *Acta Astron.*, 50, 279

Table 1. Central Coordinates of Fields Observed in NGC 0247

Field	RA(1950.0)	Dec(1950.0)
NGC 0247:F1	$00^h44^m35.4^s$	$-20^\circ55'55''$
NGC 0247:F2	$00^h44^m40.9^s$	$-21^\circ04'15''$
NGC 0247:F3	$00^h44^m33.4^s$	$-20^\circ53'11''$

Table 2. Journal of Observations of NGC 0247 Cepheid Fields

Date(UT)	Telescope	Chip	Scale	Fields	Filters
Nov. 24, 1984	CTIO	RCA	0.60 arcsec/pxl	1	<i>R</i>
Sept. 19, 1985	CTIO	RCA	0.60 arcsec/pxl	1	<i>VRI</i>
Sept. 20, 1985	CTIO	RCA	0.60 arcsec/pxl	1,2	<i>VR; VR</i>
Sept. 21, 1985	CTIO	RCA	0.60 arcsec/pxl	2	<i>BVI</i>
Sept. 22, 1985	CTIO	RCA	0.60 arcsec/pxl	1,2	<i>V; V</i>
Sept. 23, 1985	CTIO	RCA	0.60 arcsec/pxl	1,2	<i>V; V</i>
Dec. 06, 1985	CTIO	RCA	0.60 arcsec/pxl	1	<i>VR</i>
Dec. 07, 1985	CTIO	RCA	0.60 arcsec/pxl	1,2	<i>BVI; BVI</i>
Dec. 08, 1985	CTIO	RCA	0.60 arcsec/pxl	1,2	<i>VR; VR</i>
Oct. 25, 1986	CTIO	RCA	0.60 arcsec/pxl	1,2	<i>BV; RI</i>
Oct. 26, 1986	CTIO	RCA	0.60 arcsec/pxl	1,2,3	<i>VRI; BVRI; VRI</i>
Nov. 08, 1986	CTIO	RCA	0.60 arcsec/pxl	1,2	<i>BV; BV</i>
Nov. 09, 1986	CTIO	RCA	0.60 arcsec/pxl	1,2,3	<i>VRI; VRI; BVRI</i>
Sept. 24, 1987	CTIO	RCA	0.60 arcsec/pxl	1,2,3	<i>BVRI; BV; BV</i>
Oct. 13, 1987	CTIO	RCA	0.60 arcsec/pxl	1,2,3	<i>B; BVRI; BVRI</i>
Oct. 22, 1987	CTIO	RCA	0.60 arcsec/pxl	1,2	<i>BVRI; BVI</i>
Nov. 21, 1987	CTIO	RCA	0.60 arcsec/pxl	1,2	<i>BV; B, V</i>
Nov. 25, 1987	CTIO	RCA	0.60 arcsec/pxl	1,2,3	<i>VRI; VRI; VRI</i>
Sept. 10, 1988	CTIO	RCA	0.60 arcsec/pxl	1,2,3	<i>BVRI; BVRI; BV</i>
Sept. 15, 1988	CTIO	RCA	0.60 arcsec/pxl	1,2,3	<i>BVI; BV; BV</i>
Oct. 07, 1988	CTIO	RCA	0.60 arcsec/pxl	1,2,3	<i>BVRI; VRI; BVRI</i>
Oct. 13, 1988	CTIO	RCA	0.60 arcsec/pxl	1,2,3	<i>VRI; BVRI; VRI</i>
Nov. 07, 1988	CTIO	RCA	0.60 arcsec/pxl	1,2,3	<i>BV; BV; BV</i>
Sept. 10, 1991	LCO	FORD1	0.16 arcsec/pxl	1,2,3	<i>R; R; VR</i>
Sept. 11, 1991	LCO	FORD1	0.16 arcsec/pxl	1,2,3	<i>BVRI; BVRI; BVRI</i>
Sept. 12, 1991	LCO	FORD1	0.16 arcsec/pxl	1,2,3	<i>BVRI; BVRI; BVRI</i>
Sept. 13, 1991	LCO	FORD1	0.16 arcsec/pxl	1,2,3	<i>BVRI; BVRI; BVRI</i>
Sept. 14, 1991	LCO	FORD1	0.16 arcsec/pxl	1,2,3	<i>BVRI; BVRI; BVRI</i>
Oct. 02, 1992	LCO	TEK4	0.26 arcsec/pxl	1,2,3	<i>BVRI; BVRI; BVRI</i>
Oct. 03, 1992	LCO	TEK4	0.26 arcsec/pxl	1,2,3	<i>BVRI; BVRI; VRI</i>
Nov. 20, 1992	LCO	TEK4	0.26 arcsec/pxl	1,2	<i>BVRI; RI</i>

Table 2—Continued

Date(UT)	Telescope	Chip	Scale	Fields	Filters
Nov. 21, 1992	LCO	TEK4	0.26 arcsec/pxl	2,3	<i>BVR; BVRI</i>
Dec. 20, 1992	LCO	TEK3	0.23 arcsec/pxl	3	<i>BVRI</i>
Dec. 21, 1992	LCO	TEK3	0.23 arcsec/pxl	2	<i>BVRI</i>
Dec. 22, 1992	LCO	TEK3	0.23 arcsec/pxl	1,3	<i>VRI; BVRI</i>

Table 3. Positions for [MF09] Cepheids

Name	P(days)	RA (2000)	DEC (2000)
NGC 0247:[MF09] C1	65.86	00:47:10.6	-20:40:11
NGC 0247:[MF09] C2	48.53	00:47:03.8	-20:41:04
NGC 0247:[MF09] C3	48.38	00:47:10.5	-20:47:21
NGC 0247:[MF09] C4	33.23	00:47:10.1	-20:48:45
NGC 0247:[MF09] C5	30.931	00:47:03.5	-20:47:59
NGC 0247:[MF09] C6	27.785	00:47:07.6	-20:37:51
NGC 0247:[MF09] C7	26.2	00:47:01.1	-20:39:12
NGC 0247:[MF09] C8	22.3	00:47:01.1	-20:37:58
NGC 0247:[MF09] C9	20.2	00:47:01.4	-20:39:55

Table 4. Observations of C1 (P = 69.9 days)

Filter	Mag.	Error	Julian Day
<i>B</i>			
	22.23	0.03	2447441.6878
	21.82	0.02	2446407.6021
	22.30	0.04	2447120.5347
	22.45	0.04	2447472.5924
	22.23	0.04	2447090.5611
	22.66	0.05	2446728.6868
	22.71	0.10	2447414.7347
	22.57	0.09	2447419.6694
	22.71	0.08	2447062.6007
	22.24	0.06	2446743.6097
	22.03	0.04	2448510.6653
	21.98	0.02	2448511.7306
	22.01	0.03	2448512.7177
	22.04	0.03	2448513.7368
	22.46	0.09	2448946.6891
	22.39	0.09	2448898.8180
<i>V</i>			
	21.20	0.02	2447441.6847
	20.91	0.02	2446407.6208
	21.19	0.03	2447120.5403
	21.37	0.03	2447472.5979
	21.28	0.03	2447090.5708
	21.48	0.04	2446728.6819
	21.64	0.05	2447414.7306
	21.44	0.04	2447419.6653
	21.22	0.03	2447062.5917
	21.23	0.04	2446743.6229
	21.08	0.03	2448510.6576
	21.06	0.02	2448511.7323

Table 4—Continued

Filter	Mag.	Error	Julian Day
	21.06	0.02	2448512.7198
	21.10	0.02	2448513.6840
	21.26	0.02	2448946.6490
	21.40	0.03	2448898.8294
	21.41	0.03	2448897.6504
	21.03	0.06	2448514.7785
	20.92	0.02	2446406.6125
	20.10	0.02	2446408.6236
	21.18	0.03	2447124.6278
	21.19	0.04	2446743.6250
	21.51	0.03	2446729.5938
	20.95	0.03	2446328.6632
	20.92	0.02	2446329.6243
	20.88	0.03	2446331.5681
	20.89	0.04	2446332.5826
	20.87	0.02	2447447.6328
	21.36	0.05	2448978.5743
<i>R</i>	20.60	0.01	2447441.6910
	20.72	0.03	2447090.5514
	20.75	0.02	2447414.7417
	20.58	0.03	2447062.5854
	20.57	0.03	2448510.6493
	20.60	0.01	2448511.7340
	20.55	0.02	2448512.7198
	20.55	0.02	2448513.6924
	20.79	0.01	2448946.6623
	20.79	0.02	2448897.6596
	20.81	0.02	2448898.8385
	20.57	0.02	2448509.8417

Table 4—Continued

Filter	Mag.	Error	Julian Day
	20.75	0.02	2446029.5344
	20.40	0.02	2446406.6069
	20.44	0.01	2446408.6146
	20.65	0.02	2447124.6236
	20.66	0.02	2446744.6194
	20.91	0.02	2446729.5833
	20.42	0.02	2446328.6771
	20.40	0.02	2446329.6389
	20.45	0.01	2447447.6472
	20.73	0.04	2448978.6041
<i>I</i>			
	20.02	0.02	2447441.6965
	20.20	0.04	2447090.5556
	20.09	0.08	2447062.5819
	20.02	0.03	2448510.6410
	20.04	0.02	2448511.7337
	20.04	0.03	2448512.8333
	20.07	0.03	2448513.7007
	20.18	0.02	2448946.6748
	20.07	0.02	2448897.6686
	20.13	0.03	2448898.8482
	19.89	0.03	2446407.6104
	20.08	0.05	2447124.6375
	20.11	0.04	2446744.6153
	20.24	0.04	2446729.5875
	20.15	0.03	2447419.6590
	19.83	0.05	2446328.6528
	19.94	0.02	2447447.6528
	20.12	0.04	2448978.6166

Table 5. Observations of C2 (P = 48.3 days)

Filter	Mag.	Error	Julian Day
<i>B</i>			
	22.19	0.03	2447441.6878
	23.00	0.09	2447120.5347
	23.37	0.11	2447472.5924
	23.34	0.12	2447419.6694
	22.42	0.07	2447062.6007
	22.49	0.07	2448510.6653
	22.35	0.04	2448511.7306
	22.47	0.04	2448512.7177
	22.38	0.04	2448513.7368
	22.20	0.07	2448946.6891
	22.30	0.09	2448897.6395
	22.26	0.09	2448898.8180
<i>V</i>			
	21.52	0.02	2447441.6847
	21.95	0.05	2447120.5403
	22.35	0.09	2447472.5979
	22.03	0.09	2447414.7306
	22.15	0.04	2447419.6653
	21.67	0.06	2447062.5917
	21.69	0.06	2448510.6576
	21.71	0.04	2448511.7323
	21.66	0.04	2448512.7198
	21.69	0.05	2448513.6840
	21.53	0.04	2448946.6490
	21.60	0.03	2448898.8294
	21.56	0.04	2448897.6504
	21.57	0.10	2448514.7785
	21.58	0.03	2447447.6328
	22.40	0.12	2448978.5743

Table 5—Continued

Filter	Mag.	Error	Julian Day
<i>R</i>			
	21.17	0.02	2447441.6910
	21.14	0.04	2447062.5854
	21.21	0.04	2448510.6493
	21.29	0.05	2448511.7340
	21.28	0.03	2448512.7198
	21.32	0.03	2448513.6924
	21.15	0.02	2448946.6623
	21.24	0.03	2448897.6596
	21.21	0.04	2448898.8385
	21.25	0.03	2448509.8417
	21.20	0.03	2447447.6472
	21.74	0.10	2448978.6041
<i>I</i>			
	20.80	0.04	2447441.6965
	20.99	0.14	2447062.5819
	20.83	0.08	2448510.6410
	20.82	0.05	2448511.7337
	20.94	0.06	2448512.8333
	20.89	0.06	2448513.7007
	20.78	0.04	2448946.6748
	20.81	0.04	2448897.6686
	20.94	0.07	2448898.8482
	21.32	0.07	2447419.6590
	20.88	0.04	2447447.6528
	21.38	0.13	2448978.6166

Table 6. Observations of C3 (P = 44.3 days)

Filter	Mag.	Error	Julian Day
<i>B</i>			
	23.72	0.17	2447447.6618
	23.33	0.20	2448510.6931
	23.64	0.17	2448511.6833
	23.47	0.19	2448513.6597
	22.58	0.14	2448977.5926
	23.08	0.14	2448947.5667
	23.41	0.18	2448897.6799
	23.02	0.06	2446407.5903
	23.23	0.12	2447120.5535
	23.09	0.15	2446729.6028
	22.17	0.16	2447062.6222
<i>V</i>			
	22.46	0.07	2447441.6278
	22.65	0.13	2447447.6688
	22.70	0.14	2448510.7049
	22.76	0.12	2448511.6750
	22.55	0.10	2448512.7733
	22.60	0.10	2448513.7504
	21.88	0.06	2447419.6910
	21.96	0.04	2446407.5799
	22.07	0.04	2446408.5924
	22.24	0.06	2447120.5597
	22.26	0.08	2447124.6528
	22.00	0.12	2447472.6056
	22.61	0.15	2446744.6312
	22.57	0.12	2447090.5771
	22.34	0.09	2446729.5993
	21.54	0.10	2447414.7715
	22.36	0.11	2446330.6319

Table 6—Continued

Filter	Mag.	Error	Julian Day
	22.24	0.16	2446331.5819
	21.76	0.05	2447062.6278
	22.22	0.05	2448947.5213
	21.76	0.07	2448977.5428
	22.19	0.08	2448897.6872
<i>R</i>			
	21.87	0.05	2447441.6340
	22.02	0.08	2447447.6764
	22.20	0.08	2448510.7125
	22.20	0.08	2448511.6674
	22.04	0.06	2448513.7535
	21.65	0.14	2448977.5622
	21.84	0.03	2448947.5392
	21.68	0.04	2448897.6998
	21.91	0.05	2446729.6097
	22.00	0.08	2448512.6653
	22.00	0.08	2448509.8576
	21.55	0.05	2446406.5993
	21.51	0.04	2446408.5833
	21.75	0.06	2447124.6479
	22.11	0.10	2446744.6368
	21.72	0.09	2446329.6562
	21.62	0.09	2447081.5653
	21.68	0.04	2448946.7196
<i>I</i>			
	21.20	0.07	2447441.6396
	21.34	0.09	2447447.6819
	21.63	0.12	2448510.7201
	21.57	0.09	2448511.6583
	20.84	0.09	2448977.5759

Table 6—Continued

Filter	Mag.	Error	Julian Day
	21.28	0.05	2448947.5525
	20.95	0.05	2448897.7084
	21.39	0.12	2446729.6139
	21.03	0.07	2446407.6347
	21.18	0.10	2447124.6438
	21.37	0.12	2446744.6417
	21.30	0.11	2447090.5882
	21.73	0.16	2446330.6611
	21.02	0.11	2448898.8788
	21.18	0.07	2448946.7350

Table 7. Observations of C4 (P = 33.2 days)

Filter	Mag.	Error	Julian Day
<i>B</i>			
	23.10	0.09	2447447.6618
	23.29	0.12	2448510.6931
	23.33	0.10	2448511.6833
	23.62	0.17	2448513.6597
	22.82	0.15	2448977.5926
	23.34	0.18	2448947.5667
	22.88	0.10	2448897.6799
	22.04	0.12	2448898.8590
	22.40	0.05	2446407.5903
	23.19	0.13	2447120.5535
	22.58	0.11	2446743.6340
	22.60	0.10	2448898.6477
<i>V</i>			
	22.00	0.05	2447441.6278
	22.12	0.06	2447447.6688
	22.27	0.08	2448510.7049
	22.29	0.09	2448511.6750
	22.20	0.06	2448512.7733
	22.20	0.08	2448513.7504
	22.37	0.08	2447419.6868
	22.36	0.12	2447081.5562
	22.46	0.08	2447419.6910
	21.86	0.05	2446407.5799
	21.83	0.06	2446408.5924
	22.43	0.06	2447120.5597
	22.54	0.08	2447124.6528
	21.81	0.07	2447472.6056
	21.89	0.07	2446743.6403
	22.03	0.09	2446744.6312

Table 7—Continued

Filter	Mag.	Error	Julian Day
	22.62	0.10	2447090.5771
	22.45	0.08	2446729.5993
	22.00	0.09	2447414.7715
	22.41	0.10	2446329.6688
	22.41	0.08	2446330.6319
	22.57	0.18	2446331.5819
	22.74	0.12	2447062.6278
	22.44	0.05	2448947.5213
	21.83	0.07	2448898.8663
	22.27	0.12	2448977.5428
	22.05	0.06	2448897.6872
<i>R</i>			
	21.70	0.09	2447441.6340
	21.94	0.06	2448510.7125
	21.94	0.08	2448511.6674
	21.83	0.05	2448513.7535
	21.49	0.12	2448977.5622
	22.12	0.04	2448947.5392
	21.86	0.04	2448897.6998
	21.74	0.04	2448898.6209
	22.18	0.09	2446729.6097
	21.78	0.07	2448512.6653
	21.67	0.05	2448509.8576
	21.69	0.05	2446406.5993
	21.63	0.07	2446408.5833
	21.90	0.06	2447124.6479
	21.62	0.06	2446744.6368
	21.70	0.08	2447081.5653
	22.13	0.06	2448946.7196
<i>I</i>			

Table 7—Continued

Filter	Mag.	Error	Julian Day
	21.07	0.07	2447441.6396
	21.36	0.08	2448510.7201
	21.20	0.08	2448511.6583
	21.40	0.08	2448513.6340
	20.86	0.11	2448977.5759
	21.44	0.06	2448947.5525
	21.70	0.10	2448897.7084
	21.53	0.10	2448898.6084
	21.12	0.08	2446407.6347
	20.93	0.16	2447081.5694
	21.58	0.09	2448946.7350

Table 8. Observations of C5 (P = 31.0 days)

Filter	Mag.	Error	Julian Day
<i>B</i>			
	23.45	0.13	2447447.6618
	22.72	0.08	2448510.6931
	22.56	0.07	2448511.6833
	22.62	0.06	2448512.7618
	22.95	0.12	2448513.6597
	22.85	0.20	2448977.5926
	23.08	0.04	2448947.5667
	22.78	0.06	2446407.5903
	23.10	0.10	2447120.5535
	22.97	0.10	2447090.5819
	23.53	0.16	2446729.6028
	23.64	0.12	2447419.6812
	22.81	0.20	2448898.6477
<i>V</i>			
	22.76	0.08	2447441.6278
	23.15	0.12	2447447.6688
	22.28	0.08	2448510.7049
	22.28	0.08	2448511.6750
	22.27	0.07	2448512.7733
	22.17	0.06	2448513.7504
	22.89	0.10	2447419.6868
	23.06	0.16	2447419.6910
	22.21	0.06	2446406.5903
	22.21	0.05	2446407.5799
	22.33	0.06	2446408.5924
	22.35	0.06	2447120.5597
	22.38	0.08	2447124.6528
	22.74	0.18	2447472.6056
	22.42	0.11	2446743.6403

Table 8—Continued

Filter	Mag.	Error	Julian Day
	22.26	0.12	2446744.6312
	22.30	0.07	2447090.5771
	22.66	0.09	2446729.5993
	22.92	0.15	2446330.6319
	22.49	0.09	2447062.6278
	22.30	0.04	2448947.5213
	22.63	0.13	2448898.8663
	22.25	0.11	2448977.5428
	22.56	0.09	2448897.6872
<i>R</i>			
	22.32	0.09	2447441.6340
	22.55	0.09	2447447.6764
	22.06	0.07	2448510.7125
	22.01	0.07	2448511.6674
	22.05	0.06	2448513.7535
	21.91	0.17	2448977.5622
	22.03	0.04	2448947.5392
	22.37	0.07	2448897.6998
	22.58	0.08	2448898.6209
	22.34	0.09	2446729.6097
	21.85	0.06	2448512.6653
	22.00	0.06	2448509.8576
	22.04	0.07	2446406.5993
	22.09	0.06	2446408.5833
	22.10	0.08	2447124.6479
	21.99	0.08	2446744.6368
	22.44	0.12	2446329.6562
	21.93	0.04	2448946.7196
<i>I</i>			
	21.99	0.14	2447441.6396

Table 8—Continued

Filter	Mag.	Error	Julian Day
	21.78	0.12	2447447.6819
	21.47	0.08	2448510.7201
	21.41	0.08	2448511.6583
	21.53	0.08	2448513.6340
	21.51	0.17	2448977.5759
	21.61	0.06	2448947.5525
	22.04	0.14	2448897.7084
	21.78	0.14	2448898.6084
	21.94	0.21	2446729.6139
	21.55	0.11	2446407.6347
	21.74	0.18	2447124.6438
	21.49	0.15	2446744.6417
	21.56	0.12	2447090.5882
	21.63	0.14	2446330.6611
	21.53	0.07	2448946.7350

Table 9. Observations of C6 (P = 30.1 days)

Filter	Mag.	Error	Julian Day
<i>B</i>			
	22.77	0.05	2447441.6653
	22.86	0.10	2448510.7882
	23.06	0.09	2448511.6944
	22.88	0.10	2447062.6361
	22.35	0.05	2447472.6167
	23.29	0.18	2446744.6611
	22.77	0.08	2447090.6125
	22.22	0.09	2447414.8458
	22.45	0.05	2447419.7062
	22.26	0.08	2447081.6049
	22.56	0.09	2448976.6208
	22.24	0.12	2448978.6345
	22.13	0.09	2448947.6249
	22.96	0.17	2448897.7201
<i>V</i>			
	22.28	0.04	2447441.6590
	22.25	0.11	2448510.7826
	22.64	0.10	2448511.7069
	22.53	0.08	2448512.7764
	22.65	0.10	2448513.7483
	22.23	0.10	2448509.8903
	22.22	0.06	2447090.6083
	21.88	0.08	2447081.6007
	22.57	0.09	2447124.6708
	22.03	0.05	2447472.6229
	22.95	0.19	2446744.6569
	22.36	0.08	2446729.6292
	21.90	0.09	2447414.8403
	22.04	0.04	2447419.7021

Table 9—Continued

Filter	Mag.	Error	Julian Day
	22.19	0.08	2447062.6458
	21.97	0.04	2447447.7035
	22.00	0.11	2448976.6353
	21.93	0.10	2448978.6484
	21.98	0.04	2448947.5844
	22.32	0.07	2448897.7311
	22.12	0.06	2448898.6789
<i>R</i>			
	21.94	0.04	2447441.6528
	21.82	0.05	2448510.7583
	22.04	0.08	2448511.7153
	21.91	0.05	2448512.7781
	21.88	0.05	2448513.7521
	21.72	0.05	2448509.8750
	21.88	0.06	2447124.6764
	22.39	0.12	2446744.6521
	21.76	0.05	2447090.6000
	21.68	0.05	2446729.6201
	21.50	0.08	2447081.5917
	21.60	0.04	2447447.6965
	21.50	0.09	2448976.6483
	21.60	0.03	2448947.5974
	21.70	0.05	2448897.7402
	21.74	0.05	2448898.6700
<i>I</i>			
	21.54	0.08	2447441.6479
	21.59	0.11	2448510.7417
	21.38	0.07	2448511.7229
	21.66	0.12	2448513.5979
	21.55	0.06	2448512.7778

Table 9—Continued

Filter	Mag.	Error	Julian Day
	21.42	0.16	2447124.6812
	21.55	0.15	2447090.5958
	21.58	0.16	2446729.6243
	21.32	0.07	2447447.6910
	21.15	0.09	2448976.6609
	21.32	0.05	2448947.6100
	21.53	0.09	2448897.7494
	21.44	0.06	2448898.6607

Table 10. Observations of C7 (P = 26.1 days)

Filter	Mag.	Error	Julian Day
<i>B</i>			
	23.50	0.07	2447441.6878
	23.00	0.05	2446407.6021
	22.99	0.07	2447472.5924
	23.27	0.10	2447090.5611
	23.75	0.11	2446728.6868
	22.81	0.05	2447419.6694
	22.98	0.11	2446743.6097
	23.32	0.13	2448512.7121
	22.68	0.13	2448513.6222
<i>V</i>			
	23.19	0.10	2447441.6847
	22.40	0.05	2446407.6208
	22.72	0.12	2447472.5979
	22.88	0.09	2447090.5708
	22.96	0.12	2446728.6819
	22.81	0.20	2447414.7306
	22.55	0.07	2447419.6653
	22.95	0.18	2447062.5917
	22.50	0.13	2446743.6229
	22.68	0.12	2448512.7024
	22.53	0.13	2448513.6168
	23.00	0.12	2448946.6490
	23.23	0.17	2448898.8294
	22.45	0.06	2446406.6125
	22.47	0.06	2446408.6236
	23.19	0.15	2447124.6278
	22.43	0.13	2446743.6250
	23.06	0.12	2446729.5938
	22.86	0.18	2446331.5681

Table 10—Continued

Filter	Mag.	Error	Julian Day
	22.40	0.05	2447447.6328
	23.04	0.18	2448978.5743
	23.26	0.18	2448509.8903
<i>R</i>			
	22.66	0.05	2447441.6910
	22.29	0.09	2447090.5514
	22.25	0.13	2447062.5854
	22.33	0.09	2448512.6941
	22.31	0.09	2448513.6089
	22.40	0.07	2448946.6623
	22.85	0.10	2448897.6596
	22.55	0.06	2446029.5344
	22.14	0.06	2446406.6069
	22.13	0.06	2446408.6146
	22.46	0.09	2447124.6236
	22.26	0.10	2446744.6194
	22.53	0.09	2446729.5833
	22.19	0.08	2446328.6771
	22.57	0.13	2446329.6389
	22.10	0.04	2447447.6472
	22.66	0.02	2448978.6041
	22.94	0.13	2448509.8810
<i>I</i>			
	22.51	0.15	2447441.6965
	22.14	0.02	2447090.5556
	21.74	0.09	2448946.6748
	22.24	0.14	2448897.6686
	21.78	0.13	2446407.6104
	21.68	0.16	2446744.6153
	22.02	0.19	2446729.5875

Table 10—Continued

Filter	Mag.	Error	Julian Day
	21.83	0.11	2447419.6590
	21.93	0.13	2447447.6528

Table 11. Observations of C8 (P = 22.3 days)

Filter	Mag.	Error	Julian Day
<i>B</i>			
	23.76	0.09	2447441.6653
	23.57	0.11	2448511.6944
	23.97	0.02	2447062.6361
	24.18	0.02	2447472.6167
	22.63	0.10	2446744.6611
	23.84	0.18	2447090.6125
	23.65	0.13	2447419.7062
<i>V</i>			
	22.82	0.07	2447441.6590
	22.77	0.15	2448510.7826
	23.10	0.03	2448511.7069
	22.94	0.11	2448512.7764
	23.07	0.15	2448513.7483
	22.88	0.18	2448509.8903
	23.29	0.15	2447090.6083
	22.51	0.14	2447081.6007
	22.25	0.07	2447124.6708
	23.22	0.15	2447472.6229
	22.28	0.09	2446744.6569
	23.22	0.15	2446729.6292
	22.92	0.08	2447419.7021
	22.80	0.12	2447062.6458
	23.25	0.15	2447447.7035
	22.47	0.13	2448978.6484
	23.26	0.12	2448947.5844
	23.42	0.18	2448897.7311
	23.34	0.19	2448898.6789
<i>R</i>			
	22.37	0.05	2447441.6528

Table 11—Continued

Filter	Mag.	Error	Julian Day
	22.18	0.10	2448510.7583
	22.51	0.12	2448511.7153
	22.44	0.09	2448512.7781
	22.54	0.10	2448513.7521
	22.35	0.09	2448509.8750
	21.88	0.06	2447124.6764
	22.05	0.08	2446744.6521
	22.81	0.10	2447090.6
	22.53	0.10	2446729.6201
	22.32	0.16	2447081.5917
	22.62	0.08	2447447.6965
	22.04	0.14	2448978.6613
	22.94	0.12	2448947.5974
	22.62	0.10	2448897.7402
<i>I</i>			
	21.98	0.10	2447441.6479
	22.05	0.16	2448510.7417
	21.92	0.13	2448511.7229
	21.90	0.09	2448512.7778
	21.36	0.14	2447124.6812
	22.13	0.29	2446744.6479
	21.89	0.18	2446729.6243
	21.59	0.18	2447414.8340
	22.37	0.16	2447447.6910
	22.35	0.13	2448947.6100

Table 12. Observations of C9 (P= 20.2 days)

Filter	Mag.	Error	Julian Day
<i>B</i>			
	23.88	0.14	2447441.6878
	23.74	0.13	2446407.6021
	23.60	0.17	2447120.5347
	23.80	0.17	2447472.5924
	23.65	0.17	2447090.5611
	23.90	0.19	2446728.6868
	23.83	0.17	2447419.6694
	22.82	0.12	2447062.6007
	23.27	0.16	2446743.6097
	23.04	0.15	2448946.6891
<i>V</i>			
	23.25	0.11	2447441.6847
	23.31	0.14	2446407.6208
	23.27	0.18	2447120.5403
	22.73	0.12	2447472.5979
	23.06	0.15	2447090.5708
	23.18	0.13	2446728.6819
	22.84	0.19	2447414.7306
	23.35	0.16	2447419.6653
	22.49	0.12	2447062.5917
	22.81	0.17	2446743.6229
	22.49	0.06	2448946.6490
	23.26	0.16	2446406.6125
	23.40	0.17	2446408.6236
	22.53	0.11	2447124.6278
	22.69	0.15	2446743.6250
	23.46	0.20	2446729.5938
	22.60	0.07	2447447.6328
<i>R</i>			

Table 12—Continued

Filter	Mag.	Error	Julian Day
	22.86	0.10	2447441.6910
	22.63	0.18	2447090.5514
	22.62	0.12	2447414.7417
	22.40	0.15	2447062.5854
	22.43	0.06	2448946.6623
	22.41	0.07	2446029.5344
	22.87	0.15	2446406.6069
	22.91	0.14	2446408.6146
	22.36	0.10	2447124.6236
	22.48	0.15	2446744.6194
	22.72	0.12	2446729.5833
	22.75	0.16	2446329.6389
	22.30	0.06	2447447.6472

Table 13. Properties of Unclassified Variables Found in NGC 0247

ID	Field	Coordinates ^a		P(?) (days)	$\langle B \rangle$	$\langle V \rangle$	$\langle R \rangle$	$\langle I \rangle$
		x	y		σ_B	σ_V	σ_R	σ_I
NGC 0247:[MF09] P1	1	227.0	223.4	14.4	(23.49)	21.56	20.66	19.59
					0.03	0.01	0.02	0.01
NGC 0247:[MF09] P2	3	100.6	305.6	16.3	(22.59)	20.81	19.68	18.73
					0.03	0.01	0.01	0.01
NGC 0247:[MF09] P3	3	104.4	090.7	28.4	(23.53)	21.49	20.26	19.14
					0.07	0.03	0.03	0.02
NGC 0247:[MF09] P4	3	052.4	311.8	30.8	(22.84)	20.88	19.89	18.93
					0.03	0.02	0.01	0.01
NGC 0247:[MF09] P5	2	178.3	149.8	63.2	(23.10)	22.09	21.54	21.01
					0.05	0.02	0.02	0.02

^aOrigin at bottom left (south-east) corner of frame

Table 14. Properties of NGC 0247 Cepheids

ID	Field	Coordinates ^{a, b}		P (days)	$\langle B \rangle$	$\langle V \rangle$	$\langle R \rangle$	$\langle I \rangle$
		x	y		σ_B	σ_V	σ_R	σ_I
NGC 0247:[MF09] C1	1	097.8	474.5	69.9	(22.31)	21.21	20.65	20.07
					0.08	0.04	0.03	0.02
NGC 0247:[MF09] C2	1	011.6	250.5	48.3	(22.77)	21.92	21.51	21.11
					0.13	0.07	0.05	0.07
NGC 0247:[MF09] C3	2	211.7	302.1	44.3	(22.99)	21.78	21.81	21.19
					0.13	0.07	0.05	0.05
NGC 0247:[MF09] C4	2	069.4	290.9	33.2	(22.86)	22.12	21.79	21.28
					0.09	0.04	0.04	0.02
NGC 0247:[MF09] C5	2	151.1	130.1	31.0	(23.11)	22.59	22.23	21.68
					0.08	0.05	0.04	0.04
NGC 0247:[MF09] C6	3	055.5	362.2	30.1	(22.82)	22.37	21.84	21.44
					0.11	0.07	0.06	0.03
NGC 0247:[MF09] C7	1	196.9	201.3	26.1	(23.30)	22.79	22.36	22.03
					0.12	0.06	0.04	0.09
NGC 0247:[MF09] C8	3	044.7	187.1	22.3	(23.52)	22.93	22.50	22.06
					0.20	0.08	0.08	0.09
NGC 0247:[MF09] C9	1	125.4	208.0	20.2	(23.49)	22.93	22.57	...
					0.12	0.09	0.06	...

^aOrigin at bottom left (south-east) corner of frame

^bScale = 0.6 arcsec/pxl

Table 15. Revised VI Magnitudes and Updated Periods for Cepheids in NGC 0247

[MF09] ID	[GV08] ID	P (days)	$\langle V \rangle$ σ_V	$\langle R \rangle$ σ_R	$\langle I \rangle$ σ_I
NGC 0247:[MF09] C1	cep020	69.9	21.21 0.03	20.65 0.03	20.07 0.02
NGC 0247:[MF09] C2	cep017	48.3	21.92 0.07	21.51 0.05	21.11 0.07
NGC 0247:[MF09] C3	cep016	44.38	22.26 0.06	21.83 0.05	21.23 0.05
NGC 0247:[MF09] C4	cep011	33.23	22.12 0.04	21.79 0.04	21.28 0.02
NGC 0247:[MF09] C5	cep008	30.931	22.59 0.03	22.23 0.05	21.68 0.03
NGC 0247:[MF09] C6	cep005	27.785	22.42 0.03	21.77 0.06	21.65 0.03
NGC 0247:[MF09] C7		26.1	22.76 0.06	22.40 0.06	21.96 0.09
NGC 0247:[MF09] C8		22.3	22.88 0.08	22.38 0.08	21.91 0.10
NGC 0247:[MF09] C9		20.2	22.93 0.09	22.57 0.06

Table 16. Summary of Cepheid Distance Moduli to NGC 0247

Sample	No. & Bands	μ_o (σ)	D(Mpc) (σ)	E(V-I) (σ)
Original [MF09] VRI Sample	9 VRI	27.78 (0.13)	3.60 (0.22)	0.07 (0.05)
Updated [MF09] VRI Sample	9 VRI	27.81 (0.06)	3.65 (0.17)	0.07 (0.04)
Updated [MF09] VI Sample	9 VI	27.79 (0.13)	3.61 (0.23)	0.07 (0.04)
Original [GV08] VI Sample	17 VI	27.82 (0.08)	3.66 (0.14)	0.15 (0.03)
Updated [GV08] VI Sample	17 VI	27.87 (0.09)	3.75 (0.15)	0.11 (0.03)
Updated & VI Merged Sample	20 VI	27.85 (0.13)	3.72 (0.15)	0.11 (0.03)